Proc INCEMIC
Bangalore, India
10-11 Sept. 1987
pp. 43-46

IEEE Trans. EMC
1989, pp. 117-124

CIRCUIT AND ELECTROMAGNETIC SYSTEM DESIGN NOTES

Note 33

26 June 1985

THEORETICAL CONSIDERATIONS FOR OPTIMAL POSITIONING OF PEAKING CAPACITOR ARMS ABOUT A MARX GENERATOR PARALLEL TO A GROUND PLANE

D.V. Giri
Pro-Tech, 125 University Avenue, Berkeley, CA 94710
and
Carl E. Baum
Air Force Weapons Laboratory

Abstract

The object of this note is to develop theoretical considerations useful in determining the electromagnetically optimal positions for a specified number of peaking-capacitor arms about a Marx generator parallel to a ground plane. It is shown that one can determine this via a conformal transformation. Furthermore a parameter is defined and computed which is indicative of the effectiveness of the peaking-capacitor arms in shielding the Marx from the ground plane.

CONTENTS

I. INTRODUCTION

In attempting to determine the hardness of systems to a nuclear electromagnetic pulse (EMP) environment one often performs system level tests using a simulated environment [1]. There are a number of factors which influence the behavior of the simulated electromagnetic field, including the physical design of the simulator and the design of the pulsers which provide the transient energy to the simulator.

In this note, attention is focussed on certain aspects of the Marx type of pulse generator such as installed in numerous EMP simulators. Specifically, we address the problem of optimal positioning of a given number N_p of peaking capacitor arms around the central Marx column, above a perfectly conducting ground plane. After a brief discussion in the next two paragraphs of some of the background material, we conclude this introductory section with remarks about how this note is organized.

Traditionally, the pulsers for EMP simulators have been developed and built by researchers and practitioners of the science of high voltage engineering. However, it is useful to think of the pulser as a wave generator, launching a transient EM wave onto the wave guiding structure that may be represented by a suitable load. In a typical situation, the load is a two-parallel-plate transmission line type of EMP simulator, with a nominal input impedance that is dominated by the principal TEM mode of propagation. Although the simulator viewed as a transmission line can and does support the non-TEM modes, the input impedance of the simulator is still mainly governed by the TEM wave because the non-TEM modes (E (or TM) and H (or TE)) are evanascent near both ends of the simulator.

So fortunately, the load into which the pulser delivers transient energy is a quantity that is known fairly accurately and it is mainly purely resistive. Typical values for this load vary in the 100Ω to 150Ω range. By replacing the simulator per se with a resistive load, one can begin to focus attention on the various pulser components.

In general, the performance characteristics e.g., TEM, E, and H modes in cylindrical and conical regions, field mapping, terminator effectiveness of the simulator proper are much better known [1 to 6] than the performance characteristics of the pulse generator viewed as a wave generator/launcher. See [1] for a more complete bibliography concerning EMP simulators, and [7] for a review of the various pulse power systems used in EMP simulators. Also, [8] contains a survey of available Van de Graaf and Marx pulsers as well as typical parallel plate transmission-line type of simulators. Some problem areas associated with Marx pulsers have been identified and addressed in the past. An important aspect of Marx pulsers relates to the electromagnetic optimization of the relative orientation or positioning of Marx and peaking-capacitor arms. Such an electromagnetic optimization is the subject of this note. Related past work in this area [9] considered a numerical solution for optimally distributing 4 peakers around the Marx generator. We seek a generalization of this procedure with approximate answers for a large number of peakers.

After a brief description of the physical model of a typical Marx and peaker system in Section II, Section III deals with the multiconductor transmission-line model for the Marx/peaker system based on the theoretical considerations found in [10]. This is followed in Section IV by a simplified two-wire model of a Marx/peaker system. This model is obtained by essentially replacing the system of N_p number of peakers by a single effective peaker conductor. Next in Section V, the field and potential distribution for a line current or line charge over a ground plane [11, 12] is reviewed for later use. In Section VI, the optimal locations of peakers based on the two-wire model constraints are discussed, followed in Section VII by a procedure to determine the optimum peaker locations based on a conformal transformation. Simplified formulas for large values of N_p are obtained in Section VIII. This allows us to define a parameter δ which represents the undesirable coupling between Marx and ground plane through the peaking capacitor array. This is followed by an illustrative example of $N_p = 8$ and a load impedance of 150Ω. This note is concluded with a summary in Section IX followed by a list of references.

II. PHYSICAL MODEL OF PEAKERS AND MARX

The Marx type of pulser under consideration has an array of peaking capacitor arms as part of its electromagnetic configuration, which aids in delivering transient energy to the EMP simulator. An idealized Marx generator driving a conical wave launcher is shown in figure 2.1a. The Marx/peaker is typically connected via suitable transitions to an output switch near the apex end and to the wave launching section of the transmission-line type of EMP simulator on the output end. A cross-sectional view showing the Marx generator and the peaker arms distributed around it is also shown in figure 2.1b. The problem at hand is to determine the optimal locations of a specified number of peakers in a given cross section. Typically, the Marx column is approximately elliptical and a peaker arm is rectangular in their cross sections. However, it is desirable to model the Marx generator and the peaker arms by circular cylindrical conductors with appropriate per-unit-length transmission line parameters. Additional distributed elements may be included if need be e.g., series Marx inductance L'_M can be added to the per-unit-length transmission line inductance. In the remainder of this section, ways of modelling the Marx column and a typical peaker arm are discussed.

1. Marx generator model

A typical Marx column consists of a series of individual capacitor trays with associated charging and triggering circuit elements and the individual Marx switch. Although the Marx might be approximated as elliptical in cross section, it is convenient to choose a circular conductor model for purposes of analysis. At least 3 models appear possible to represent the Marx generator as follows:

(a) a line current at the geometrical center of the Marx as shown in figure 2.2 (which can represent the current going

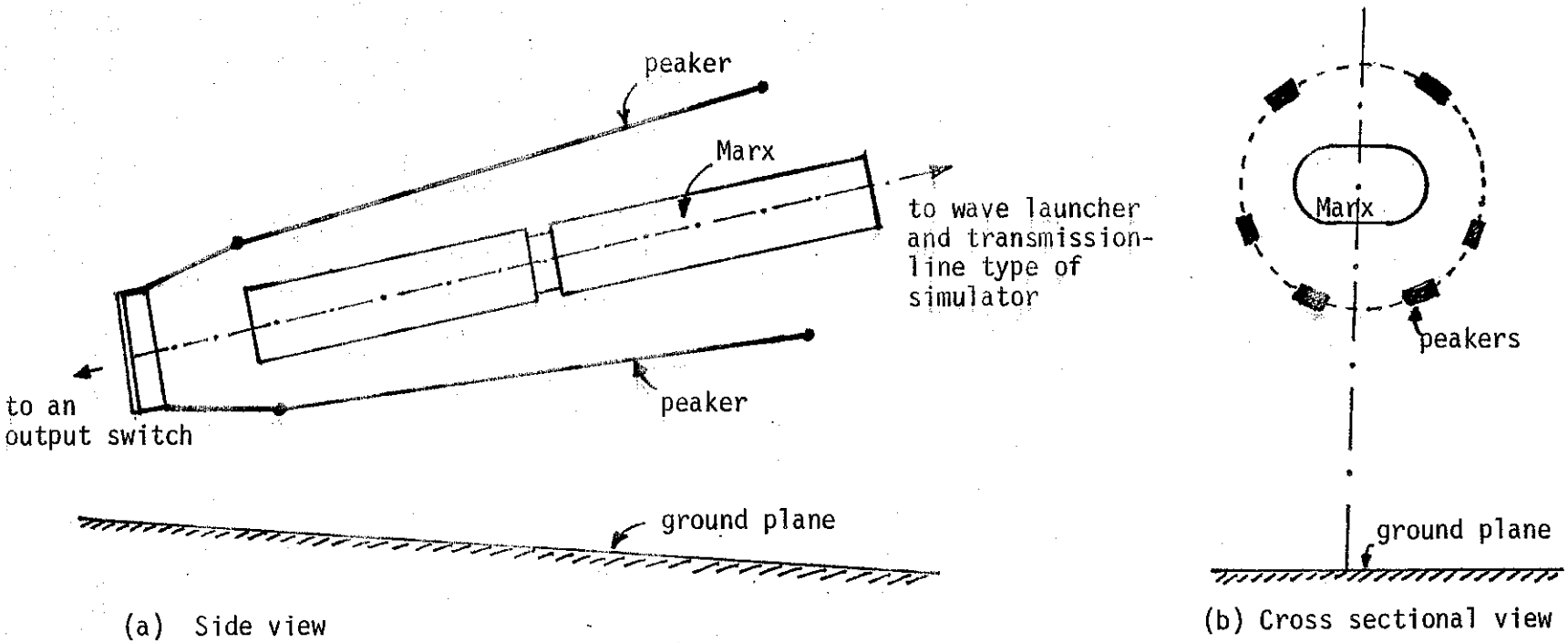

Figure 2.1 Two views of Marx/peaker system above a ground plane.

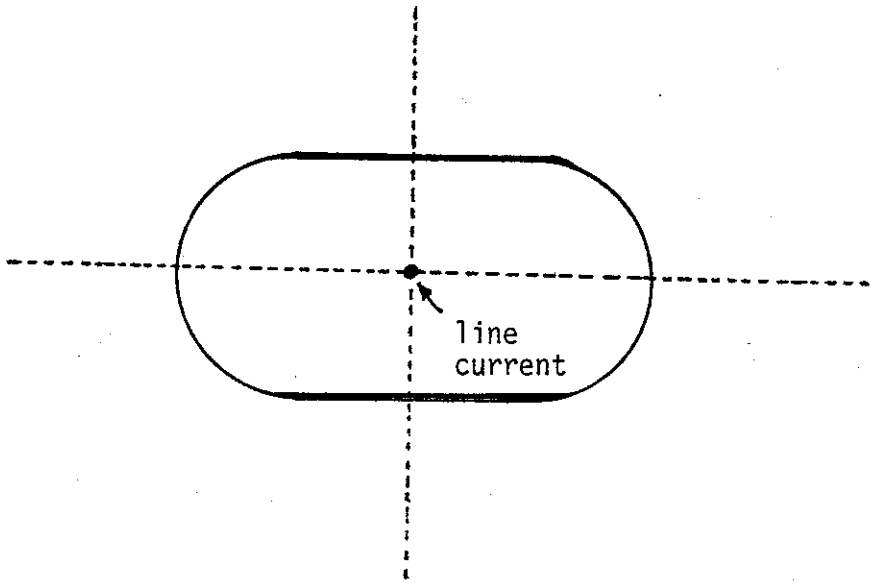

Figure 2.2 Line current model of Marx column.

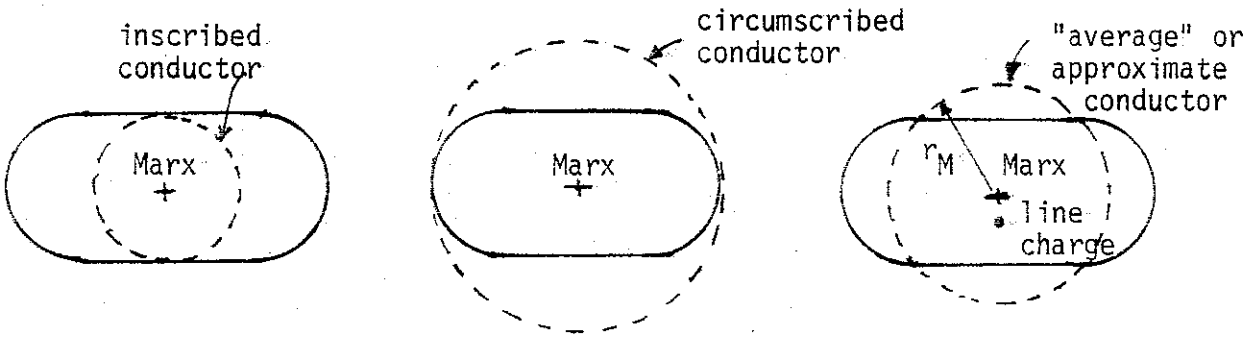

(a) inscribed circle (b) circumscribed circle (c) average circle

Figure 2.3 Cylindrical conductor model for the Marx column and a line charge that renders the "average" Marx conductor an equipotential.

through the Marx switches and capacitors with average position in the center);

(b) a line charge so placed as to make the "average" Marx conductor an equipotential as in figure 2.3 (which allows the charge to be distributed nonuniformly around the Marx (typically on grading rings) so as to more closely match that appropriate to the exterior geometry);

(c) two line charges so placed as to make the approximately elliptical outer boundary of the Marx an equipotential as in figure 2.4.

Models (b) and (c) above rely on the fact that placing a conductor on an equipotential surface does not alter the field and potential distribution from a line current or charge. It is further noted that the "average" Marx conductor has a radius r_M which can be approximated as an average of the radii of the inscribed and circumscribed circles, as seen in figure 2.3. The line current at the geometric center is accurate for estimating the per-unit-length inductance parameters, whereas the line charge models yield accurate capacitance per unit length parameter. Model (b) above is sufficiently accurate for the present purposes and can be used with an added Marx inductance L'_M. It is also emphasized that such a model is strictly valid in a cross section i.e., if the Marx generator is sloping with respect to the ground plane, the equivalent-line-charge model will also be sloping. This process of obtaining the line charge is illustrated in figures 2.5, 2.6 and 2.7. Basically, one obtains the height of the line charge at any two cross sections to arrive at the sloping line charge. The net result of the sloping Marx generator is that one has to determine the optimal peaker locations at least in two cross sections and slope the peakers also accordingly. This is of interest in practice, whereas the theoretical considerations can be demonstrated in a cross section.

2. Peaker-arm model

The peaking capacitor arms used in conjunction with typical Marx generators serve the function of masking the inductance of the Marx and thereby provide a peaking element in achieving a fast rise time pulse into a transmission line type of EMP simulator. Each arm consists of several unit peaking capacitors

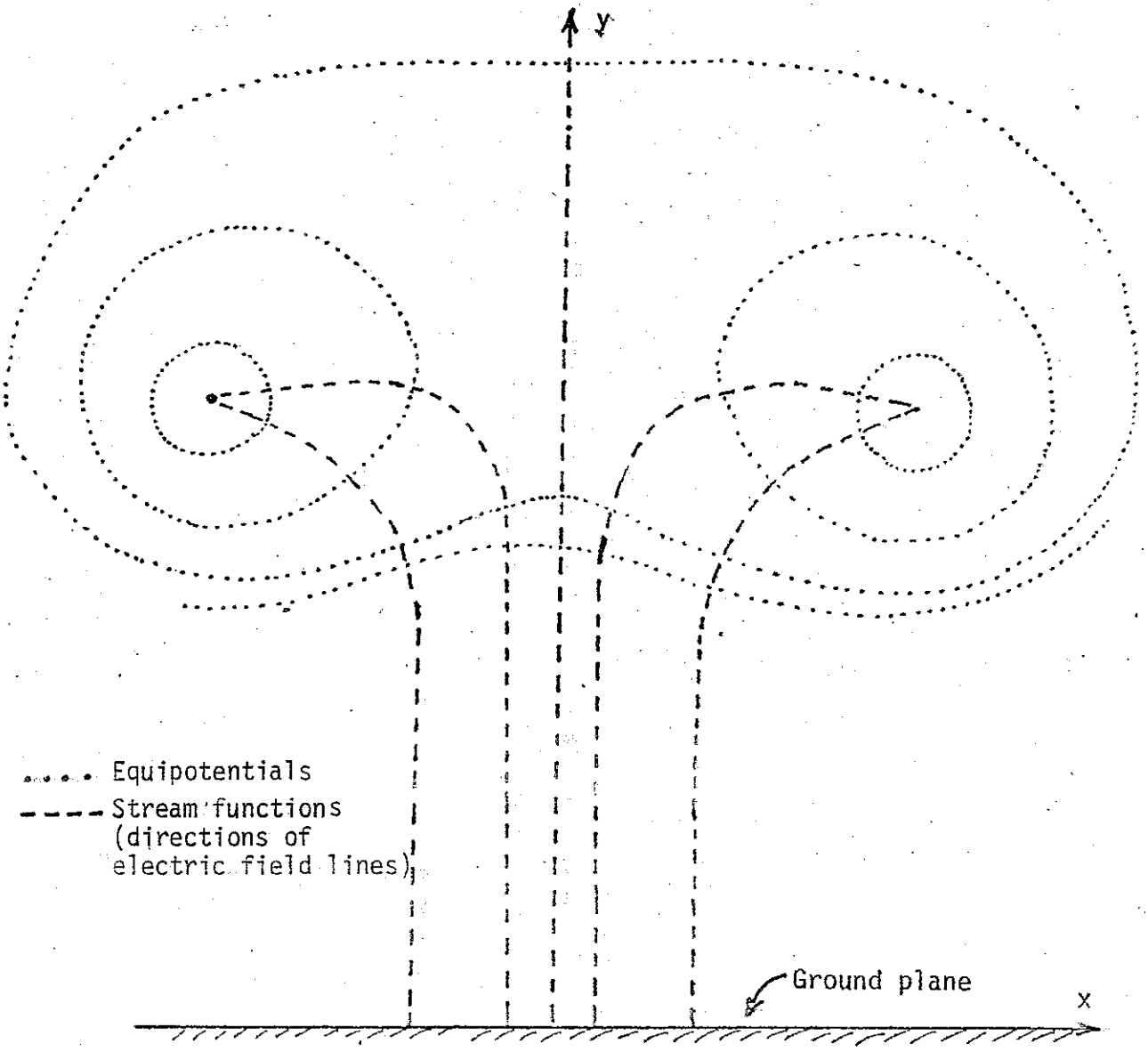

Figure 2.4 Two line charges model for the Marx column that renders the approximate elliptical outer boundary of the Marx an equipotential.

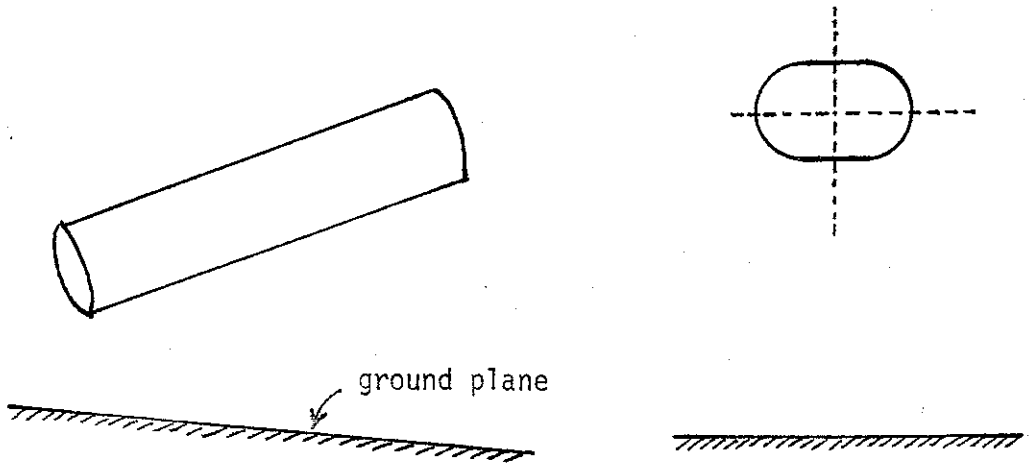

Figure 2.5 Marx generator with an elliptic cross section sloping above a ground plane.

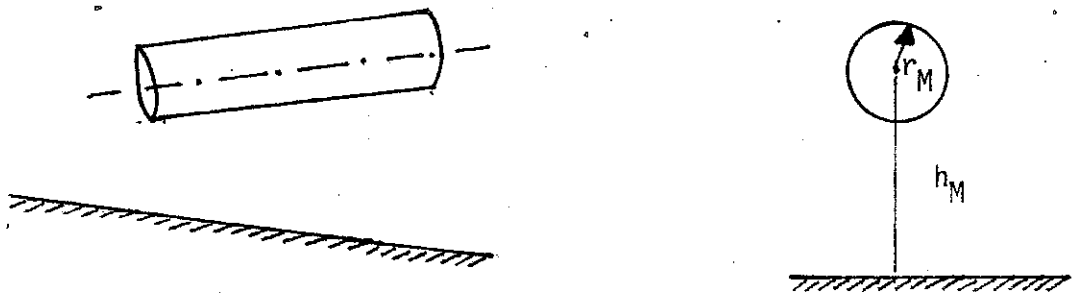

Figure 2.6 Equivalent "average" cylindrical Marx conductor.

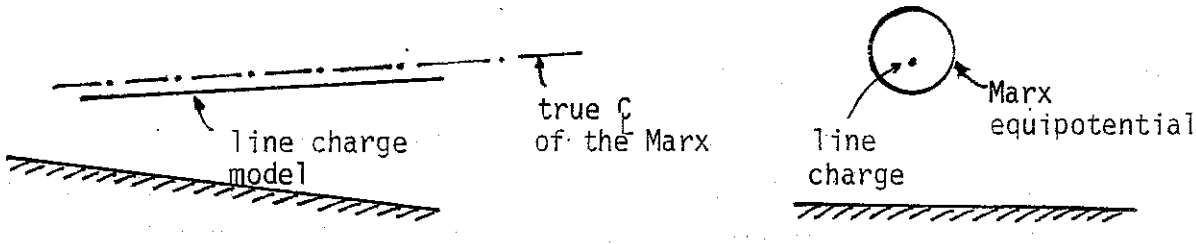

Figure 2.7 Sloping line charge model for the sloping Marx generator.

connected in series, each of which in turn contains a series string of the elemental or the basic pad capacitors. Typical shape of a unit peaking capacitor is shown in figure 2.8 and an equivalent cylindrical conductor model for an individual peaker arm is developed in figures 2.9 and 2.10.

In concluding this section, it is noted that the typical cross sectional shapes of Marx generators and peaker arms are non-circular, but approximate circular cylindrical models which give an equivalent radius are possible as illustrated. Note that the average used in figure 2.10 is not the only or most accurate equivalent radius. The present result is quite accurate if $h << w$ or conversely, since it is given the well-known result for a strip. Such models with equivalent radii are useful in later sections dealing with the question of optimal peaker distributions about the Marx generator.

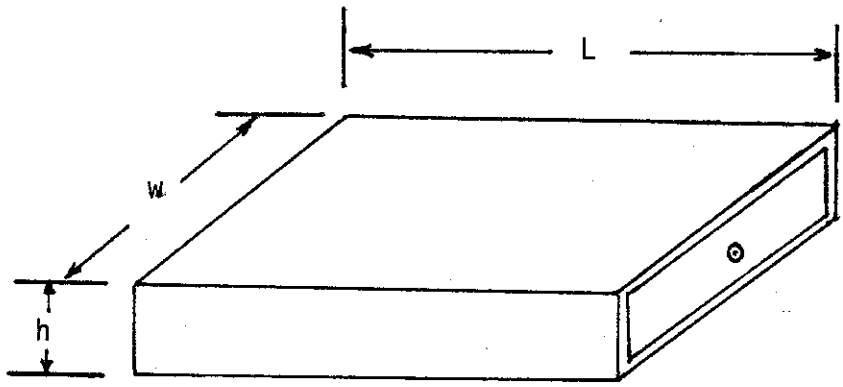

Figure 2.8 Typical shape of a unit peaking capacitor
e.g., dimensions L = 50 cm, w = 10 cm, h = 5 cm.

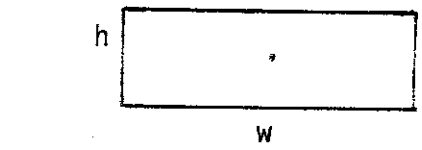

Figure 2.9 Cross section of a peaker arm.

Figure 2.10 Cylindrical conductor model for a peaker arm.

III. MULTICONDUCTOR TRANSMISSION-LINE MODEL FOR MARX AND PEAKERS

The central Marx column along with the surrounding peaking capacitor arms over a ground plane form a multiconductor transmission line. Consequently, a multiconductor transmission line model of the Marx and N_p number of peaking capacitor arms is useful in analyzing the wave transport properties. Some of the relevant considerations from the general theory of multiconductor transmission lines [10] are summarized below.

The analysis of the transmission-line networks described in [10] is based on the network excitation from lumped or distributed voltage and current sources located at source positions along each transmission-line section (tube). Such a specification of sources is useful for the present application of the Marx/peaker system.

For review purposes, consider an N-conductor plus reference transmission line as shown in figure 3.1. N could be equal to (N_p+1) in the present application and the (N+1)th conductor is taken as the reference and it is also the image plane. The starting point of the derivation of voltages and currents is the familiar set of 2N transmission-line equations

$$\frac{d}{dz}\left(\tilde{V}_n(z,s)\right) = -\left(\tilde{Z}'_{n,m}(s)\right)\cdot\left(\tilde{I}_n(z,s)\right) \tag{3.1}$$

$$\frac{d}{dz}\left(\tilde{I}_n(z,s)\right) = -\left(\tilde{Y}'_{n,m}(s)\right)\cdot\left(\tilde{V}_n(z,s)\right) \tag{3.2}$$

where $\tilde{V}$ and $\tilde{I}$ denote voltage and current in the complex-frequency s-plane, $\vec{1}_z$ is the direction of positive current flow, $\left(\tilde{Z}'_{n,m}\right)$ and $\left(\tilde{Y}'_{n,m}\right)$ are respectively the per-unit-length longitudinal impedance and transverse admittance matrices. If there are source terms, the right hand sides of (3.1) and (3.2) are modified by the addition of $\left(\tilde{V}_n^{(s)}(z,s)\right)$ and $\left(\tilde{I}_n^{(s)}(z,s)\right)$ respectively where the superscript (s) denotes source vectors.

In the special case of a lossless transmission line consisting of perfect conductors embedded in lossless, dispersionless media

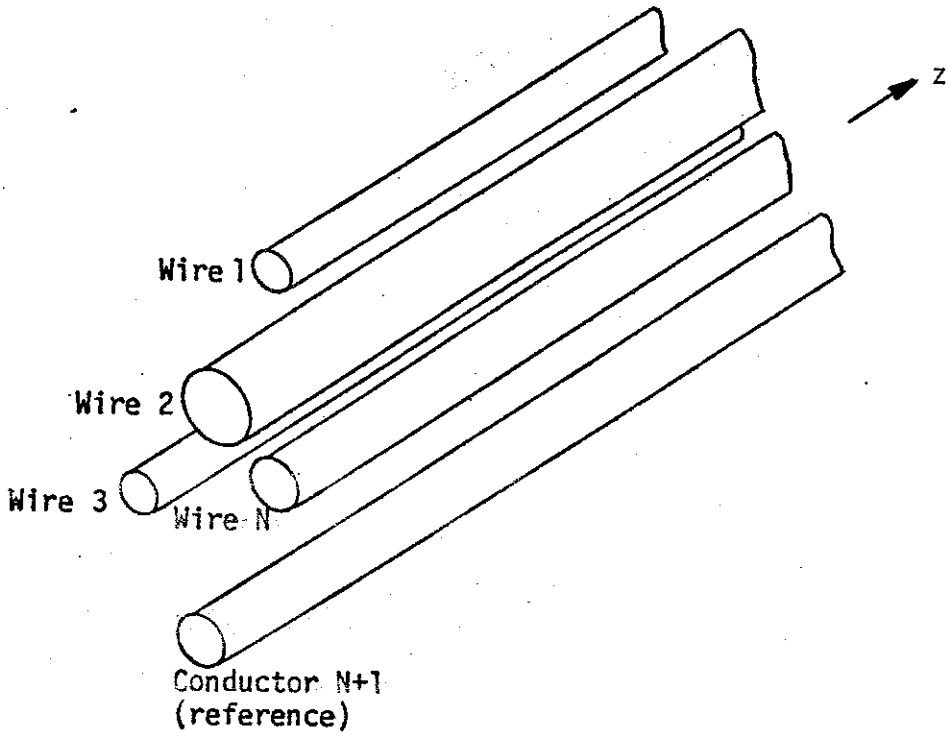

Figure 3.1 Section of a general (N+1) conductor transmission line.

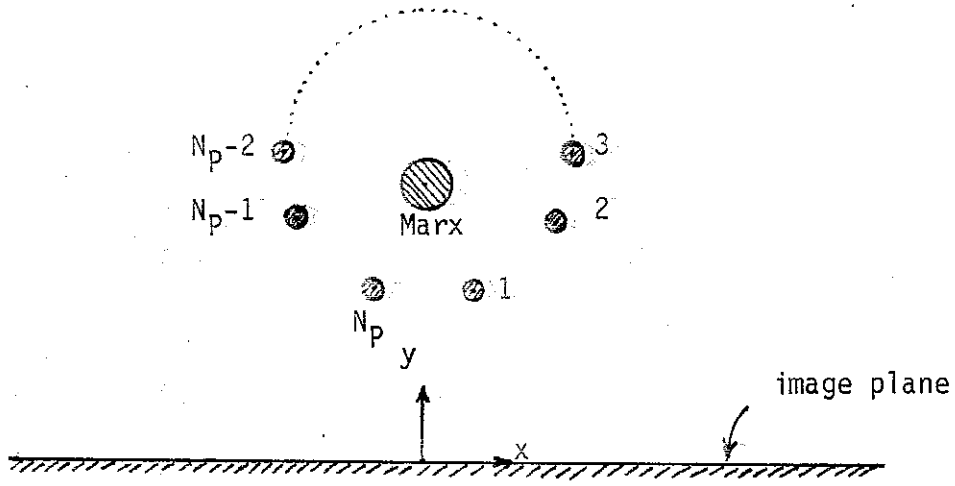

Figure 3.2 Marx generator with its N_p peaker arms above a ground plane viewed as N- conductor transmission line plus reference: $N = N_p+1$

$$\left(\tilde{Z}'_{n,m}(s)\right) = s\left(L'_{n,m}\right)$$
$$\left(\tilde{Y}'_{n,m}(s)\right) = s\left(C'_{n,m}\right) \tag{3.3}$$

where

$$\left(L'_{n,m}\right) = \text{per-unit-length inductance matrix}$$
$$\left(C'_{n,m}\right) = \text{per-unit-length capacitance matrix} \tag{3.4}$$

which are assumed to be dispersionless and, hence, constant matrices.

Recall that the squared quantity of the propagation matrix $\left(\tilde{\gamma}_{c_{n,m}}(s)\right)$ is equal to the product of the two matrices according as

$$\left(\tilde{\gamma}_{c_{n,m}}(s)\right)^2 = \left(\tilde{Z}'_{n,m}(s)\right) \cdot \left(\tilde{Y}'_{n,m}(s)\right) \tag{3.5}$$

where the square root is taken in the p.r. sense as the positive square root of non-negative eigenvalues of the right hand product. Then the characteristic impedance matrix can be found via

$$\left(\tilde{Z}_{c_{n,m}}(s)\right) = \left(\tilde{\gamma}_{c_{n,m}}(s)\right) \cdot \left(\tilde{Y}'_{n,m}(s)\right)$$
$$= \left(\tilde{\gamma}_{c_{n,m}}(s)\right)^{-1} \cdot \left(\tilde{Z}'_{n,m}(s)\right) \tag{3.6}$$

Numerous formulae, including the above, are discussed in more detail in [10].

The above equations may now be specalized for the Marx/peaker system of conductors. Owing to the presence of the additional series inductance L'_M of the Marx, which the peaker arms are designed to mask, the longitudinal-impedance-per-unit-length matrix takes the form

$$\left(\tilde{Z}'_{n,m}(s)\right) = s\mu \left(f_{g_{n,m}}\right) + s\, L'_M$$

$$= s\mu \begin{pmatrix} f_{g_{1,1}} & \cdots & f_{g_{1,N_p+1}} \\ \vdots & & \vdots \\ f_{g_{N_p+1,1}} & \cdots & f_{g_{N_p+1,N_p+1}} \end{pmatrix}$$

$$+ s\, L'_M \left(1_{n,N_p+1} \quad 1_{N_p+1,m}\right) \tag{3.7}$$

A supermatrix notation [10] can be introduced in writing (3.7) above as follows

$$\left(f_{g_{n,m}}\right) = \left(\left(f_{g_{n,m}}\right)_{u,v}\right)$$

$\equiv$ geometric factor supermatrix (for u and v = 1,2)

$$\left(f_{g_{n,m}}\right)_{1,1} \equiv (N_p \times N_p) \text{ matrix representing the peakers} \tag{3.8}$$

$$\left(f_{g_{n,m}}\right)_{2,2} \equiv (1 \times 1) \text{ matrix representing the Marx}$$

$$\left(f_{g_{n,m}}\right)_{1,2} \equiv (N_p \times 1) \text{ matrix representing the peaker/Marx interaction}$$

$$\left(f_{g_{n,m}}\right)_{2,1} \equiv (1 \times N_p) \text{ matrix representing the Marx/peaker interaction}$$

We also have

$$\left(\tilde{Y}'_{n,m}(z,s)\right) = s\varepsilon \left(f_{g_{n,m}}\right)^{-1} \tag{3.9}$$

with μ and ε being respectively the permeability and permittivity of the medium in which the multiconductor transmission line is immersed (assuming a uniform medium).

Note that if only reciprocal media are used (which is certainly the case with most dielectrics) then for both capacitance and inductance purposes, the matrices are symmetric, i.e.

$$\begin{aligned}
\left(\tilde{Z}'_{n,m}(s)\right) &= \left(\tilde{Z}'_{n,m}(s)\right)^T \\
\left(\tilde{Y}'_{n,m}(s)\right) &= \left(\tilde{Y}'_{n,m}(s)\right)^T \\
\left(f_{g_{n,m}}\right)_{1,1} &= \left(f_{g_{n,m}}\right)^T_{1,1} \\
\left(f_{g_{n,m}}\right)_{2,1} &= \left(f_{g_{n,m}}\right)^T_{1,2} \\
\left(f_{g_{n,m}}\right)_{1,2} &= \left(f_{g_{n,m}}\right)^T_{2,1}
\end{aligned} \tag{3.10}$$

$T \equiv$ matrix transpose

From purely geometrical considerations, one can write down the elements of the geometric factor matrix as [13] (assuming thin conductors),

$$f_{g_{n,m}} = \begin{cases} \frac{1}{2\pi} \ln\left(\frac{2y_n}{r_n}\right) & \text{for } n = m \\ \frac{1}{2\pi} \ln\left(\frac{d^{(i)}_{n,m}}{d_{n,m}}\right) & \text{for } n \neq m \end{cases} \tag{3.11}$$

for n and m = 1, 2 . . . . . N_p where as shown in figure 3.3

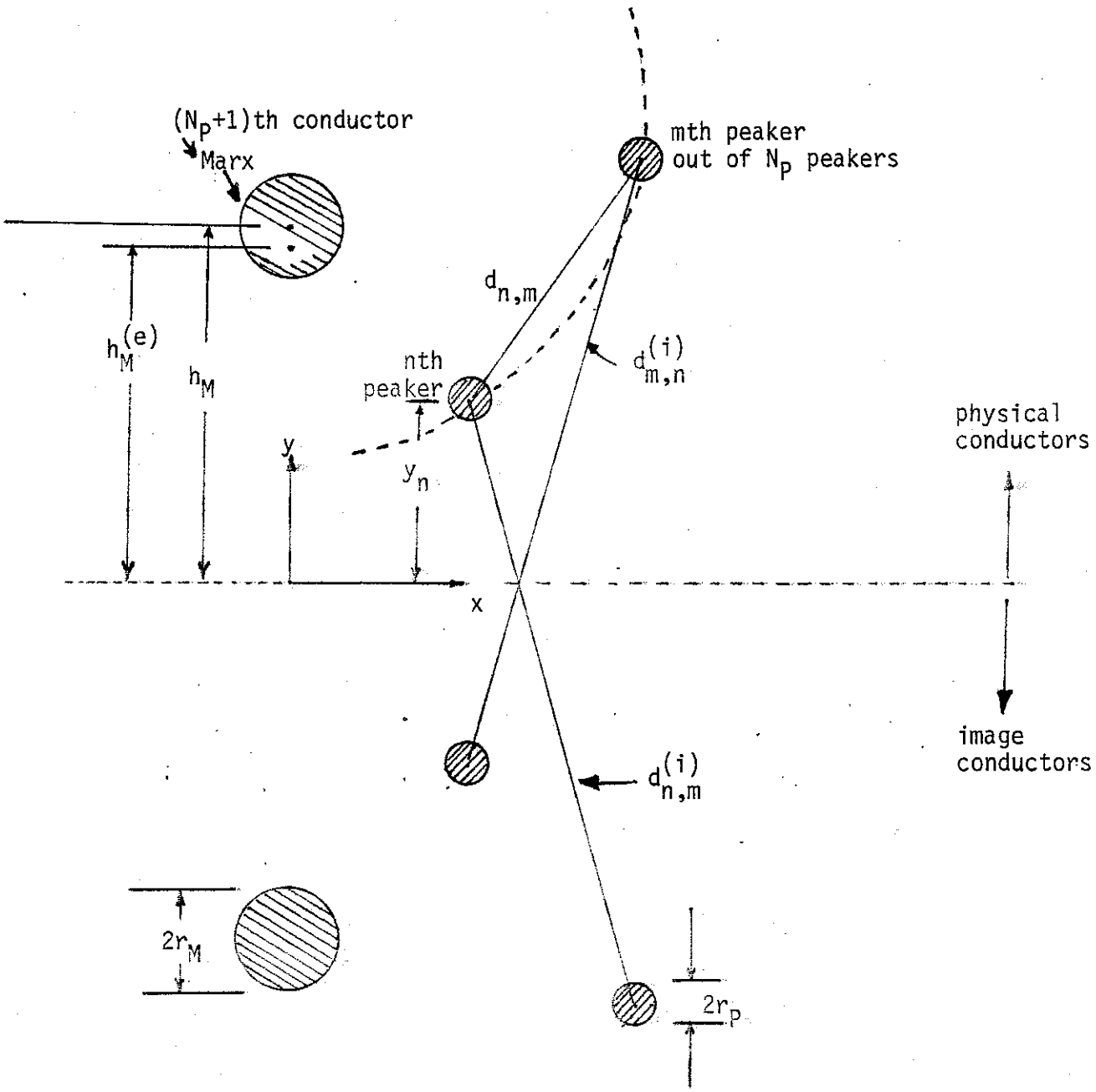

Figure 3.3 Geometrical distances useful in evaluating matrix elements.

y_n = height of the nth peaker above ground plane

$d_{n,m} = d_{m,n}$ = distance between the centers of the nth and mth conductors

$d^{(i)}_{m,n} = d^{(i)}_{n,m}$ = distance between the centers of the mth conductor and the nth image conductor = distance between the centers of the nth conductor and the mth image conductor

r_{PA} = common radius of peaker arms (3.12)

r_M = radius of Marx for capacitance purposes

h_M = height of Marx

$h^{(e)}_M$ = height of the line charge modelling the Marx, for later use

The remaining matrix elements are given by

$$f_{g_{n,N_p+1}} = \frac{1}{2\pi} \ln\left(\frac{d^{(i)}_{n,N_p+1}}{d_{n,N_p+1}}\right) \tag{3.13}$$

for $n = 1, 2 \ldots\ldots N_p$

and lastly

$$f_{g_{N_p+1,N_p+1}} = \frac{1}{2\pi} \ln\left(\frac{2h^{(e)}_M}{r_M}\right) \tag{3.14}$$

Recall that while r_M is the Marx radius for capacitive purposes, the same radius can be used for inductance parameters by the addition of an extra series inductance L'_M as already described earlier, so the f_g parameters are based on capacitive considerations.

These are the general relationships between the voltages and currents on peakers and Marx conductors. However, certain physical considerations apply during the peaker charge cycle and after the closure of the output switch in a typical Marx pulser. These considerations lead to simplifications as described in the following section.

IV. DESIRED TWO-WIRE TRANSMISSION-LINE MODEL OF MARX AND PEAKERS

In the preceeding section, the interrelationships between the voltages and currents as a function of position and frequency on the Marx/peaker system were outlined via the use of per-unit-length longitudinal impedance and transverse admittance matrices. It is the purpose here to specialize these equations under the applicable physical considerations.

Recall that in a shorthand notation, we had

$$\frac{d}{dz}\begin{pmatrix}(\tilde{V}_n(z,s))_1\\(\tilde{V}_n(z,s))_2\end{pmatrix}$$

$$= -\left[s\mu\begin{pmatrix}(f_{g_{n,m}})_{1,1} & (f_{g_{n,m}})_{1,2}\\(f_{g_{n,m}})_{2,1} & (f_{g_{n,m}})_{2,2}\end{pmatrix} + sL_M^i\begin{pmatrix}(0_{n,m})_{1,1} & (0_{n,1})_{1,2}\\(0_{1,m})_{2,1} & (1)_{2,2}\end{pmatrix}\right]$$

$$\odot\begin{pmatrix}(\tilde{I}_n(z,s))_1\\(\tilde{I}_n(z,s))_2\end{pmatrix} \qquad (4.1)$$

$\odot \equiv$ generalized dot product

where we have partitioned the vectors and matrices in a fashion compatible with the previous partition of the geometric factor matrix [14].

Since our interest is in determining the optimum peaker locations, rather than detailed voltage or current waveforms, it is adequate to focus attention on either of the two transmission-line equations. In the above '2 x 2' notation,

subscript 1 refers to N_p peakers and subscript 2 refers to Marx, as before. Next we require that the following conditions be satisfied

a) current $\tilde{I}_M$ in the Marx should produce equal $\frac{d\tilde{V}}{dz}$ in all peakers

b) voltage V_M on the Marx should produce equal $\frac{d\tilde{I}}{dz}$ in all peakers

c) equal currents in all peakers should produce equal $\frac{d\tilde{V}}{dz}$ in all peakers

d) equal voltages on all peakers should produce equal $\frac{d\tilde{I}}{dz}$ in all peakers.

Conditions (a) and (c) above are applicable on the $\frac{d\tilde{V}}{dz}$ equation (4.1) and conditions (b) and (d) above would apply to a corresponding $\frac{d\tilde{I}}{dz}$ equation. Let us investigate the implications of conditions (a) and (c) on (4.1).

Condition (a)

Setting the peaker currents to zero, i.e.

$$(\tilde{I}_n)_1 = (0_n)_1$$

$$(\tilde{I}_n)_2 = \tilde{I}_M \quad \text{(scalar quantity)} \tag{4.2}$$

and inserting these into (4.1)

$$\frac{d}{dz}(\tilde{V}_n)_1 = -s\mu \left(f_{g_{n,m}}\right)_{1,2} \tilde{I}_M$$

$$= -s\mu \left(f_{g_{n,m}}\right)^{(T)}_{2,1} \tilde{I}_M \quad \text{(by symmetry)} \tag{4.3}$$

Requiring all the peaker voltages to be the same (as functions of z and s),

$$(1_n)\ \frac{d\tilde{V}_P}{dz} = -s\mu\ f_{g_{PM}}\ (1_n)\ \tilde{I}_M \tag{4.4}$$

(1_n) = N_P component vector of 1s

Equal $(d\tilde{V}/dz)$ on all peakers imply that the left side of (4.4) is constant and, consequently all $f_{g_{n,m}}$ coupling peakers and Marx are required to be the same $f_{g_{PM}}$ as indicated. This condition using (3.11) leads to

$$\frac{1}{2\pi}\ \ell n \left(\frac{d^{(i)}_{n,N_P+1}}{d_{n,N_P+1}}\right) = \text{constant} \tag{4.5}$$

$$\left(\frac{d^{(i)}_{n,N_P+1}}{d_{n,N_P+1}}\right) = \text{constant}$$

leading to the requirement that the peakers be located at centers (x_n, y_n) of figure 3.3 such that

$$\left[\frac{x_n^2 + (y_n - h_M^{(e)})^2}{x_n^2 + (y_n + h_M^{(e)})^2}\right] = [\text{same for all } n = 1, 2 \ldots\ldots N_p \text{ peakers}] \tag{4.6}$$

It is noted that all (x_n, y_n) from above lie on a circle and, the parameter $h_M^{(e)}$ in (4.6) is the height of the Marx above the ground plane.

Condition (c)

The second condition is that equal peaker currents should produce equal $d\tilde{V}/dz$ in all peakers. Setting equal peaker currents and zero Marx current, we have

$$(\tilde{I}_n)_2 = I_M = 0$$

$$I_n = I_{PA} \text{ for } n = 1, 2, \ldots\ldots N_P \qquad (4.7)$$

$$= \text{same current in every peaker arm}$$

Inserting the above into (4.1), we have

$$\frac{d}{dz}(\tilde{V}_n)_1 = -s\mu \left(f_{g_{n,m}}\right)_{1,1} \cdot (\tilde{I}_n)_1 \qquad (4.8)$$

Requiring the voltages on the left as before to be all the same leads to

$$(1_n)\frac{d\tilde{V}_P}{dz} = -s\mu \left(f_{g_{n,m}}\right)_{1,1} \cdot (1_n)\, I_{PA} \qquad (4.9)$$

The requirement that the left side of (4.9) be the same for all peakers implies that the sum of all elements in any row of $\left(f_{g_{n,m}}\right)$ be the same. In other words

$$\sum_{m=1}^{N_P} f_{g_{n,m}} = [\text{same for all } n = 1, 2 \ldots\ldots N_P] \qquad (4.10)$$

By symmetry, it also means

$$\sum_{n=1}^{N_P} f_{g_{n,m}} = [\text{same for all } m = 1, 2 \ldots\ldots N_P] \qquad (4.11)$$

Note as discussed in [15] all the $f_{g_{n,m}}$ are positive so that the sum is positive also. Using (3.13) and (3.14) in (4.11) we have

$$\sum_{m=1}^{N_p} f_{g_{n,m}} = \sum_{m=1}^{N_p} \frac{1}{2\pi} \ln\left(\frac{d^{(i)}_{n,m}}{d_{n,m}}\right)$$

$$= \frac{1}{4\pi} \sum_{m=1}^{N_p} \ln\left(\frac{(x_n - x_m)^2 + (y_n + y_m)^2}{(x_n - x_m)^2 + (y_n - y_m)^2}\right)$$

$$= \frac{1}{4\pi} \ln\left[\prod_{m=1}^{N_p} \frac{(x_n - x_m)^2 + (y_n + y_m)^2}{(x_n - x_m)^2 + (y_n - y_m)^2}\right]$$

$$= [\text{same for all } n = 1, 2 \ldots\ldots N_p] \tag{4.12}$$

The above restriction leads to the requirement that the product quantity in rectangular parentheses above be independent of n, recalling that (x_n, y_n) is the location of the center of the nth peaker.

One could also have started with the $(d\tilde{I}/dz)$ equation, applied the other two conditions i.e., (b) and (d) and arrived at an equivalent set of constraints for N_p peaker locations. In the interest of brevity and simplicity, this has not been carried out here.

It is seen that, under the simplifying constraints above, we have a situation, provided that the boundary values at the ends of lines are also consistent with equal peaker voltages and currents, wherein

$$\frac{d}{dz}\begin{pmatrix} \tilde{V}_{PA}\,(1_n)_1 \\ \tilde{V}_M\,(1_n)_2 \end{pmatrix} = -\left[s_\mu \left(\left(f_{g_{n,m}}\right)_{u,v}\right) + s L'_M \begin{pmatrix} (0_{n,m})_{1,1} & (0_{n,m})_{1,2} \\ (0_{n,m})_{2,1} & (1_{n,m})_{2,2} \end{pmatrix}\right] \odot \begin{pmatrix} \tilde{I}_{PA}\,(1_n)_1 \\ \tilde{I}_M\,(1_n)_2 \end{pmatrix} \tag{4.13}$$

$$\frac{d}{dz}\begin{pmatrix}\tilde{I}_{PA}\,(1_n)_1\\ \tilde{I}_M\,(1_n)_2\end{pmatrix} = -s\varepsilon\left(\left(f_{g_{n,m}}\right)^{-1}_{u,v}\right)\cdot\begin{pmatrix}\tilde{V}_{PA}\,(1_n)_1\\ \tilde{V}_M\,(1_n)_2\end{pmatrix} \tag{4.14}$$

are satisfied.

In the above u and v take on the values of 1 and 2. Writing out the f_g matrix appearing above,

$$\left(\left(f_{g_{n,m}}\right)_{u,v}\right) = \begin{pmatrix}\left(f_{g_{n,m}}\right)_{1,1} & f_{g_{PM}}\,(1_n)_{1,2}\\ f_{g_{PM}}\,(1_n)_{2,1} & f_{g_M}\,(1_{1,1})_{2,2}\end{pmatrix} \tag{4.15}$$

Under equal peaker voltages $V_{PA} = V_p$, i.e., the same voltage V_p on all peakers,

$$\frac{d}{dz}\begin{pmatrix}\tilde{V}_p(z,s)\\ \tilde{V}_M(z,s)\end{pmatrix} = -\left[su\begin{pmatrix}f_{g_p} & f_{g_{PM}}\\ f_{g_{PM}} & f_{g_M}\end{pmatrix} + s\begin{pmatrix}0 & 0\\ 0 & L'_M\end{pmatrix}\right]\cdot\begin{pmatrix}\tilde{I}_p\\ \tilde{I}_M\end{pmatrix} \tag{4.16}$$

$$\tilde{I}_p = N_p\,\tilde{I}_{PA}$$

where $\tilde{I}_p$ is the total peaker current.

Expanding out the first of (4.16)

$$\frac{d}{dz}\;\tilde{V}_p(z,s) = -su\left\{\underbrace{\left[\sum_{m=1}^{N_p} f_{g_{n,m}}\right]}_{\text{any } n}\frac{\tilde{I}_p}{N_p} + f_{g_{PM}}\,\tilde{I}_M\right\} \tag{4.17}$$

$$\frac{d}{dz}\ \tilde{V}_M(z,s) = -\left[s\mu \left(\underbrace{\sum_{n=1}^{N_P}}_{\text{any } m} f_{g_{n,m}} \right) \frac{\tilde{I}_P}{N_P} \right] - \left[s\mu\, f_{g_M} + sL'_M \right] \tilde{I}_M \tag{4.18}$$

If we identify

$$f_{g_P} \equiv \underbrace{\frac{1}{N_P} \sum_{n=1}^{N_P}}_{\text{any } m} f_{g_{n,m}} = \underbrace{\frac{1}{N_P} \sum_{m=1}^{N_P}}_{\text{any } n} f_{g_{n,m}} \tag{4.19}$$

we have

$$\frac{d}{dz}\ \tilde{V}_P = -s\mu \left[f_{g_P}\ \tilde{I}_P + f_{g_{PM}}\ \tilde{I}_M \right] \tag{4.20}$$

$$\frac{d}{dz}\ \tilde{V}_M = -s\mu \left[f_{g_P}\ \tilde{I}_P + \left(f_{g_M} + \frac{L'_M}{\mu} \right) \tilde{I}_M \right]$$

Corresponding to the above, one has the $d\tilde{I}/dz$ equations, which may be formally written down as

$$\frac{d}{dz} \begin{pmatrix} \tilde{I}_P \\ \tilde{I}_M \end{pmatrix} = -s\varepsilon \begin{pmatrix} f_{g_P} & f_{g_{PM}} \\ f_{g_M} & f_{g_M} \end{pmatrix}^{-1} \cdot \begin{pmatrix} \tilde{V}_P \\ \tilde{V}_M \end{pmatrix} \tag{4.21}$$

Equations (4.20) and (4.21) above clearly display the desired two-wire model of the Marx/peaker system. The quantities that the symbols in the above pair of equations stand for are recalled and summarized below.

$\tilde{V}_P(z,s)$ ≡ equal peaker voltages

$\tilde{I}_P(z,s) = N_P \tilde{I}_{PA}(z,s)$ ≡ total peaker current

dz ≡ incremental length along propagation direction

s ≡ complex frequency $= \Omega + j\omega$

$\tilde{V}_M(z,s)$ ≡ Marx voltage

$\tilde{I}_M(z,s)$ ≡ Marx current

μ ≡ permeability of the medium $= \mu_o$ for free space

f_{g_P} ≡ peaker geometric factor

$$= \frac{1}{N_P} \sum_{m=1}^{N_P} f_{g_{n,m}} \quad \text{for any } n, \text{ as in (4.13)}$$

$$= \frac{1}{4\pi N_P} \ln \left[\prod_{m=1}^{N_P} \frac{(x_n - x_m)^2 + (y_n + y_m)^2}{(x_n - x_m)^2 + (y_n - y_m)^2} \right] \qquad (4.22)$$

$$f_{g_{PM}} = \frac{1}{4\pi} \ln \left[\frac{x_n^2 + (y_n^2 - h_M^{(e)})^2}{x_n^2 + (y_n^2 + h_M^{(e)})^2} \right] \equiv \text{geometric factor between Marx and } \underline{\text{any}} \text{ peaker (independent of } n)$$

(x_n, y_n) ≡ coordinate of the center of the nth peaker

N_P ≡ number of peaker arms

$\tilde{I}_{PA}$ ≡ individual peaker arm current $= \tilde{I}_{PA}/N_P$

$$f_{g_M} = \frac{1}{2\pi} \ln\left(\frac{2h_M^{(e)}}{r_M}\right) \equiv \text{geometric factor for Marx}$$

$h_M^{(e)}$ = height of the line charge representing the Marx center

r_M = effective radius of Marx for capacitive considerations which is also used for inductive considerations with an added series inductance L_M' per unit length

In conclusion, we have formulated the equations necessary for determining the centers (x_n, y_n) of all N_p peakers, as well as arrived at a desired two-wire model for the Marx/peaker system. Such a two-wire model is useful in studying wave transport characteristics across the Marx/peaker assembly.

However, an alternate approach based on conformal transformation is also possible for determining the optimum peaker locations. In the following Section V, we review the field and potential distribution of a line charge or current before applying it to the problem at hand.

V. FIELD AND POTENTIAL DISTRIBUTION FOR A LINE CURRENT OR CHARGE OVER A GROUND PLANE

Figure 5.1 shows the geometry of a line current or charge over a ground plane. The wire carrying the current or charge is of radius a and located at a height b above a ground plane. The cross-sectional plane is the x-y plane and the direction of wave propagation along the equivalent two-wire transmission line is in the positive z direction. The object is to obtain the potential and stream function profiles. The solution to this classical problem is available in the literature [11, 12], and it is shown in figure 5.2 and briefly discussed. The solution is for a line charge or current and a suitable equipotential could be made to coincide with the actual physical conductor. The line current or charge solution is based on a conformal transformation of the physical plane $\zeta = x' + jy'$ into a complex potential plane $w = u + jv$ where u = electric potential (volts) and v = magnetic potential (amps) and $(-dw/d\zeta)$ will yield complex fields. The relevant equations [12] are reproduced below

$\zeta \equiv$ complex variable for the physical plane = $x' + jy'$
$w \equiv$ complex variable for the potential plane = $u + jv$
u = constant is an equipotential (= magnetic field line)
v = constant is an electric field line (= magnetic potential or stream function)

$$w = \ln\left(\frac{\zeta + j}{\zeta - j}\right) = 2j \operatorname{arccot}(\zeta)$$
$$\zeta = j \coth(w/2) \qquad (5.1)$$

corresponding to a pair of line currents or charges at $(0, \pm 1)$ carrying equal and opposite currents or charges per unit length. All lengths are normalized by b_o which is the height of the line current or charge above the ground or image plane. Expanding (5.1) gives

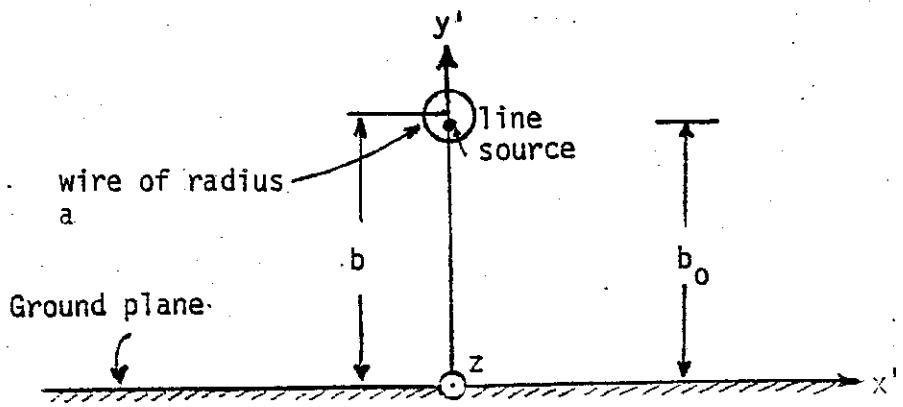

Figure 5.1 Line current or line charge above a ground plane.

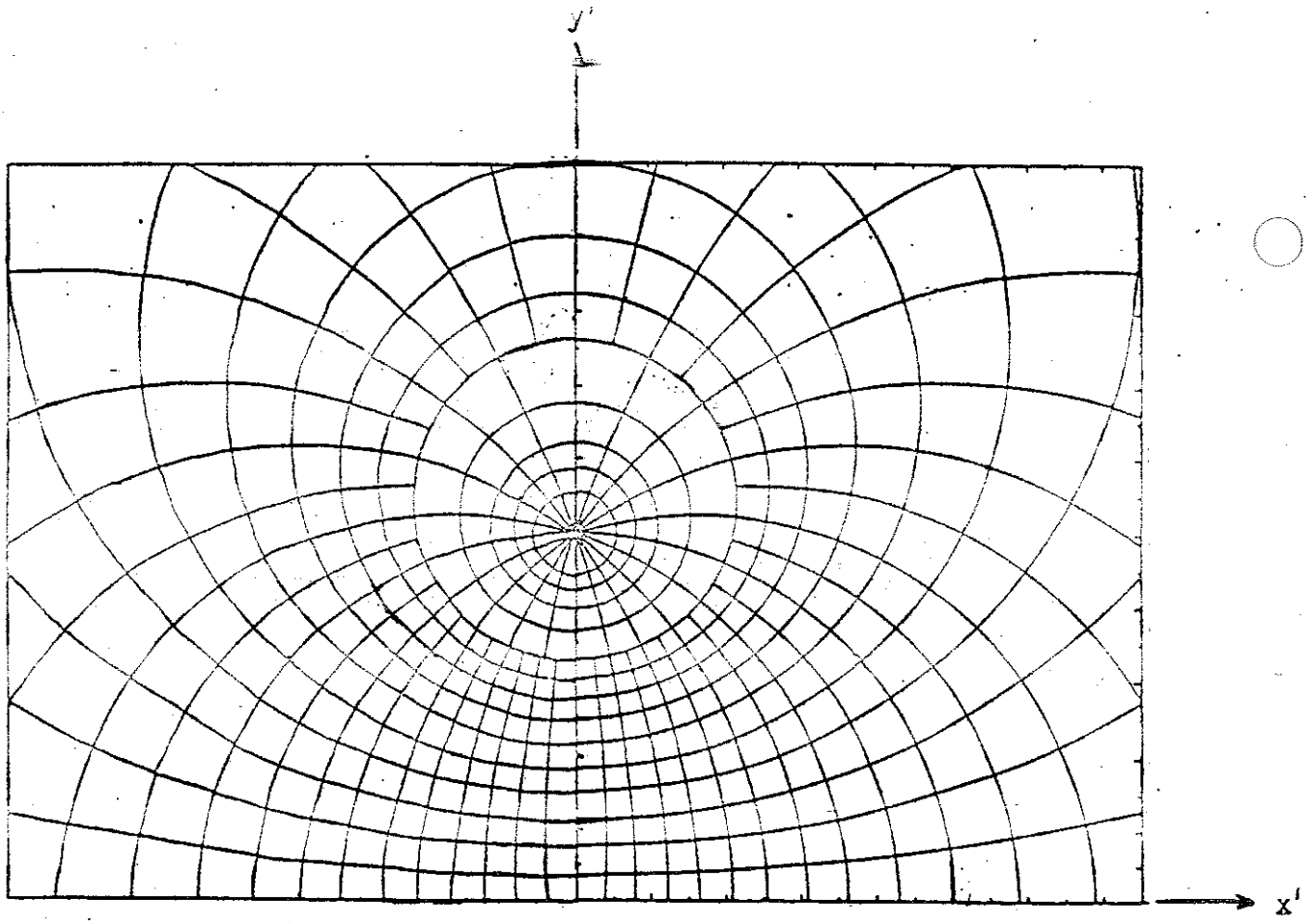

Figure 5.2 Stream function and potential distribution for the line current or line charge above a ground plane.

$$u = \frac{1}{2} \ln \left[\frac{x'^2 + (1 + y')^2}{x'^2 + (1 - y')^2} \right]$$

$$v = \arctan \left[\frac{2x'}{x'^2 + y'^2 - 1} \right] \qquad (5.2)$$

$$x' = \frac{\sin (v)}{\cosh (u) - \cos (v)}$$

$$y' = \frac{\sinh (u)}{\cosh (u) - \cos (v)}$$

The line current or charge is located such that the circle of radius a is an equipotential corresponding to the conductor. The contours of constant u and v shown in figure 5.2 are obtained from (5.2). Furthermore, it can be shown that the equipotential $u = u_0$ is a circle with a normalized center b' and normalized radius r'_c given by

$$b' = \coth (u_0); \; r'_c = \operatorname{csch} (u_0) \qquad (5.3)$$

with

$$(b/r_c) = (b'/r'_c) = \cosh (u_0) \qquad (5.4)$$

This completes a review of the potential and field distribution of a line current or charge above a ground plane. This distribution of fields and potentials is used later in Section VII for determining the optimal locations of a specified number of peaker arms.

VI. OPTIMAL PEAKER LOCATIONS BASED ON TWO-WIRE-MODEL CONSTRAINTS

The constraints on the two-wire model lead us to the following, as one may recall

$$f_{g_{n,N_p+1}} = f_{g_{N_p+1,m}} = f_{g_{PM}}$$

$$\frac{1}{N_p} \sum_{n=1}^{N_p} f_{g_{n,m}} = \frac{1}{N_p} \sum_{m=1}^{N_p} f_{g_{n,m}} = f_{g_p} \tag{6.1}$$

Put differently, the N_p peakers should be placed such that the f_g parameters between the Marx and <u>any</u> peaker is the same. In addition, the peakers should be placed such that the sum of the elements of any row of the peaker f_g matrix does not depend on the row. By symmetry, this is also true for columns. Mathematically, these two constraints become

$$\frac{1}{4\pi} \ln\left(\frac{x_n^2 + (y_n - h_M^{(e)})^2}{x_n^2 + (y_n + h_M^{(e)})^2}\right) = \left\{\begin{matrix}\text{same constant for all} \\ n = 1, 2 \ldots\ldots N_p\end{matrix}\right\}$$

$$\frac{1}{4\pi} \sum_{m=1}^{N_p} \ln\left(\frac{(x_n - x_m)^2 + (y_n + y_m)^2}{(x_n - x_m)^2 + (y_n - y_m)^2}\right) = \left\{\begin{matrix}\text{same constant for all} \\ n = 1, 2 \ldots\ldots N_p\end{matrix}\right\} \tag{6.2}$$

where $\bar{h}_M^{(e)}$ is the effective height of the Marx above the ground plane. The unknowns in (6.2) are (x_n, y_n) for $n = 1, 2 \ldots N_p$. In other words there are $2\,N_p$ unknowns (i.e. N_p number of xs and N_p number of ys) and there are enough equations in (6.2) to solve for (x_n, y_n) in terms of a single (x_n, y_n) that could be arbitrary. Efficient numerical schemes could be devised to solve the coupled set of (6.2). One such scheme is below.

Step 1. Select one peaker at location (x_1, y_1).

Step 2. Compute $f_{g_{PM}}$ for it using

$$f_{g_{1,M}} = \frac{1}{4\pi} \ln\left(\frac{x_1^2 + (y_1 - h_M^{(e)})^2}{x_1^2 + (y_1 + h_M^{(e)})^2}\right) \tag{6.3}$$

Step 3. Evaluate (N_p-1) differences as

$$\Delta_i^{(PM)} = \left(f_{g_{i,M}} - f_{g_{1,M}}\right) \quad \text{for } i = 2 \ldots\ldots N_p$$

$$= \frac{1}{4\pi}\left[\ln\left(\frac{x_i^2 + (y_i - h_M^{(e)})^2}{x_i^2 + (y_i + h_M^{(e)})^2}\right) - \ln\left(\frac{x_1^2 + (y_1 - h_M^{(e)})^2}{x_1^2 + (y_1 + h_M^{(e)})^2}\right)\right] \tag{6.4}$$

Step 4. Evaluate and minimize the quantity

$$\sum_{i=2}^{N_p} \left[\Delta_i^{(PM)}\right]^2 \to 0 \tag{6.5}$$

Step 5. Similarly

$$\sum_{i=2}^{N_p} \left[\Delta_i^{(P)}\right]^2 \to 0 \tag{6.6}$$

where

$$\Delta_i^{(P)} = \frac{1}{4\pi}\left[\sum_{m=1}^{N_P} \ell n\left(\frac{(x_i - x_m)^2 + (y_i + y_m)^2}{(x_i - x_m)^2 + (y_i - y_m)^2}\right) - \sum_{m=1}^{N_P} \ell n\left(\frac{(x_1 - x_m)^2 + (y_1 + y_m)^2}{(x_1 - x_m)^2 + (y_1 - y_m)^2}\right)\right] \tag{6.7}$$

Out of the minimization of processes in steps 4 and 5 above, come the location of the (N_P-1) centers (x_n, y_n) for $n = 2, 3 \ldots\ldots N_P$ in terms of an arbitrary (x_1, y_1).

This formally completes the procedure for obtaining the optimal peaker locations for a specified number N_P of them, based on the constraints applicable on a two-wire transmission-line model for the Marx/peaker assembly.

VII. OPTIMAL PEAKER LOCATIONS BASED ON CONFORMAL TRANSFORMATION

Earlier in Section V, the potential and stream function of a line current or charge above a ground plane was reviewed. The object of this section is to apply those results in determining the optimal locations of a specified number N_P of peakers, each of effective radius r_{PA}. The Marx generator column is modelled by a circular cylinder of effective radius r_M. In other words, the height of the line current or charge above the ground plane is chosen such that the "average" Marx conductor is an equipotential.

Referring to figure 2.7 for example, it is seen that the Marx column could be sloping, resulting in varying heights of Marx at different cross sections. This calls for the analysis in at least two cross sections. But the procedure of obtaining peaker locations could be illustrated in a cross section, and applied at several cross sections as needed.

In a given cross section, one first determines the height of the line current or charge using (5.3) and (5.4). In this cross section, one chooses a particular equipotential to distribute the peakers. The procedure is outlined below and illustrated in figure 7.1. Recall that we need equal peaker voltages, which means the individual peaker arms lie on an equipotential surface caused by the line current or charge modelling the Marx.

The we follow the following procedure:

(a) normalize all distances to Marx line current or line charge height so that this line is located at $x' = 0$ and $y' = +1$.

(b) determine the desired geometric factor f_p given by

$$f_p = Z_p / Z \quad \text{where} \tag{7.1}$$

Z_p = impedance of peaker array to ground plane

Z = characteristic impedance of the medium = $\sqrt{\mu/\varepsilon}$

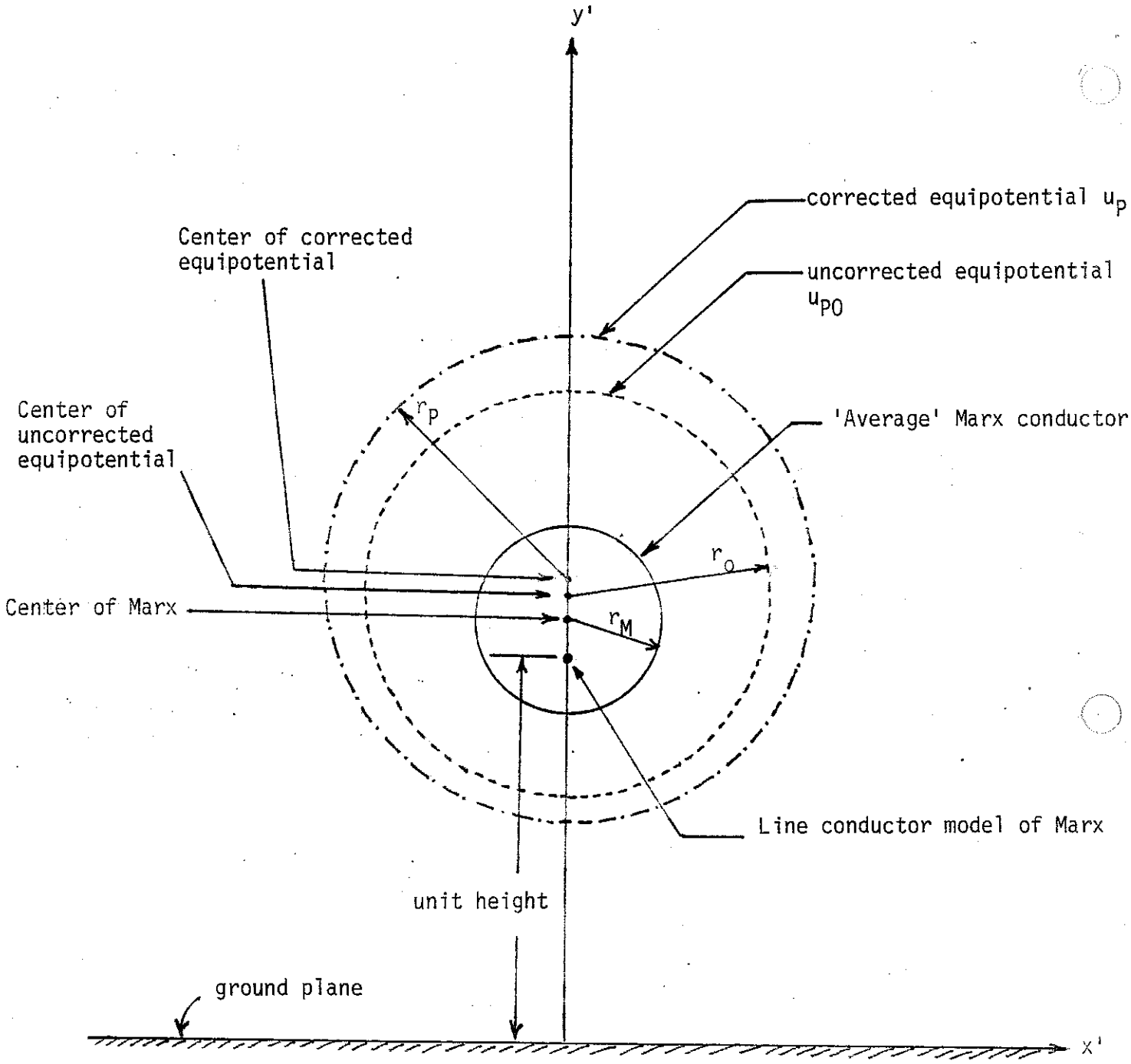

Figure 7.1 Determination of the equipotential surface upon which N_p peakers will be distributed in the normalized physical plane ($\zeta = x' + jy'$).

(c) the desired geometric factor f_p will then correspond to a desired equipotential

$$u_{P0} = 2\pi f_{P0} \quad \text{(see footnote below)} \tag{7.2}$$

(d) the height b_o of the center of and, radius r_o of the desired equipotential are given by

$$b_o = \coth(u_{P0})$$
$$r_o = \operatorname{csch}(u_{P0}) \tag{7.3}$$

(e) specify the number of peakers N_p

(f) For the given N_p, compute a correction term Δr in the radius of the equipotential u_{P0}, resulting from the fact that a finite number of 'rods' is approximating a continuous surface. Using a planar approximation [16], this correction is given by

$$\Delta r \cong \left[\frac{\text{half the peaker spacing}}{\pi}\right] \times \ell n \left[\frac{\text{peaker spacing}}{\pi \times \text{peaker diameter}}\right] \tag{7.4}$$

For the peaker spacing, one may use the average spacing given by

$$\text{peaker spacing} \cong \frac{1}{N_p}\left(\begin{matrix}\text{circumference of the uncorrected or the}\\ \text{desired equipotential}\end{matrix}\right)$$
$$= 2\pi\, r_o/N_p \tag{7.5}$$

which results in

$$\Delta r \cong \frac{r_o}{N_p} \ell n\left(\frac{r_o}{N_p r_{PA}}\right) \tag{7.6}$$

(g) The corrected equipotential then has a radius given by

$$r_p = r_o + \Delta r \tag{7.7}$$

and the corrected equipotential corresponding to r_p is

$$u_p = \operatorname{arccsch}(r_p)$$
$$f_p = u_p/(2\pi) \tag{7.8}$$
$$\Delta f_p = (u_{P0} - u_p)/(2\pi)$$

The f_g parameters in this note are referenced to ground plane, whereas reference [12] is for the full transmission line. Hence the factor of two.

(h) On this corrected equipotential u_p we distribute the N_p peakers such that they all carry equal currents = I_{PA}. If the total current on the peaker 'cylinder' is I_p, one may divide the cylinder into sections carrying equal currents. Each section is then replaced by a peaker arm implying that the Δv between adjacent peakers on the corrected equipotential be the same. This approximation gets better with increasing value of N_p. So, one chooses the first peaker at $v = v_1$, based on symmetry about the y' axis, then the remainder of (N_p-1) peakers are chosen according as

$$v_n = v_1 + \left[\frac{2\pi n}{N_p}\right] \qquad (7.9)$$

for $n = 1, 2, 3, \ldots\ldots (N_p-1)$

Step (h) above may be described in some additional detail. It is noted that the peakers are distributed on the corrected equipotential in a manner which makes Δv = constant = $(2\pi/N_p)$ between adjacent peakers. This arrangement ensures approximately equal currents in all of the N_p peaker arms during the peaker charge cycle, as well as during the discharge following the closure of the output switch. Imagine that the peaker arms actually were replaced by a circular perfectly conducting cylindrical shell given by u_p = constant. Then the distribution of the surface current density and surface charge density is given by the stream function v. This applies separately both outside and inside the cylindrical shell, since this imaginary shell is a shield. Taking equal Δv corresponds to equal currents and charges per unit length. In the center of each Δv the current and charge per unit length is accumulated on a peaker arm, and if Δv is sufficiently small (or N_p is sufficiently large) this represents a small perturbation. Note equal currents and charge per unit length require equal impedances in the arms, specifically the capacitance - length products of these arms should all be the same.

It is also recognized that for both odd and even values of N_p, two choices are possible for positioning the peakers as illustrated in figure 7.2, while still maintaining a constant Δv increment and symmetry with respect to the y axis.

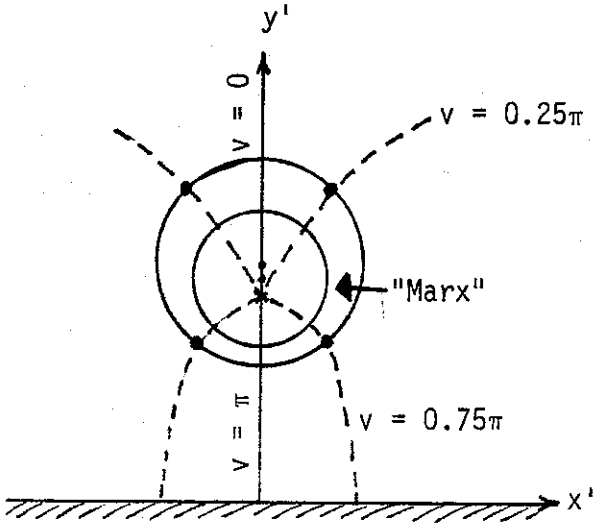

(Preferred)

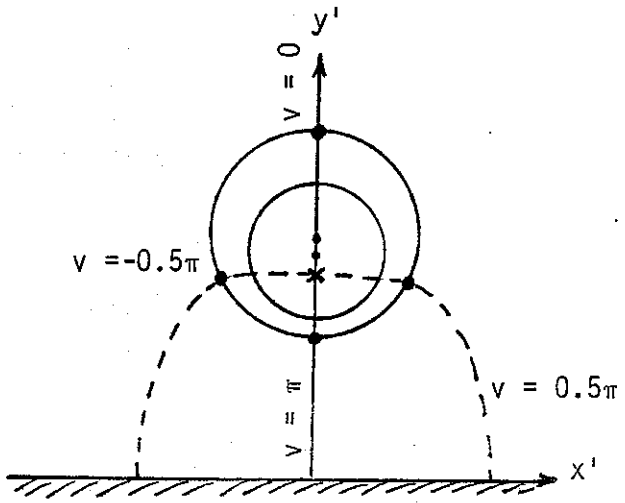

(a) N_p even (= 4 say)

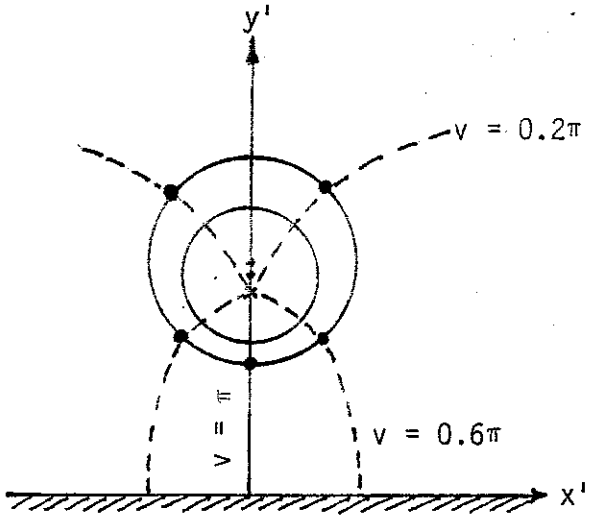

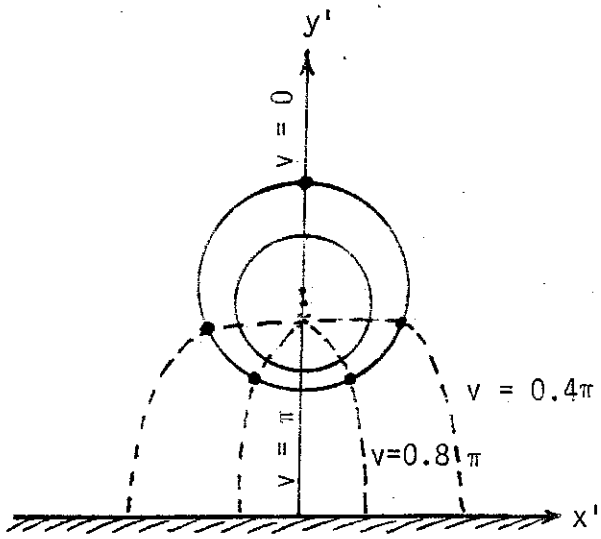

(Preferred)

(b) N_p odd (= 5 say)

Figure 7.2 Two possible choices for peaker distribution, based on symmetry, each for N_p even and odd.

For the case of N_p = even, one can have no peakers on the y' axis or 2 on the y' axis as in figure 7.2a. For the case of N_p = odd, one can have one peaker on the y' axis, either directly above or below the Marx generator as in figure 7.2b. In both cases the preferred configuration resulting in the largest minimimum separation between peaker arms and a circular Marx cross section are indicated. For a circular Marx cross section this minimizes average electric fields and resulting electrical breakdown problems. Note that real Marx cross sections are not necessarily circular.

It is also recalled that the choice of a particular equipotential u_p ensures that the transmission line formed by the "peaker cage" and the ground plane matches the characteristic impedance of the principal TEM mode of propagation. Matching the impedance and ensuring equal currents during both the peaker charge cycle and discharge cycle, is the essence of this electromagnetic optimization.

VIII. APPROXIMATE SOLUTION FOR LARGE N_p WITH AN ILLUSTRATIVE EXAMPLE

As N_p increases, the peaker cage begins to resemble a cylindrical tubular conductor about the Marx. The radius and height of this "tube" are governed by impedance matching considerations. As N_p increases, the correction to the desired equipotential may be neglected. With reference to figure 7.1,

$$r_p \cong r_o$$

$$f_p = Z_p/Z \tag{8.1}$$

$$u_p \cong u_{p0} \cong 2\pi f_p$$

On this equipotential, one distributes the N_p peakers according as

$$v_n = v_1 + \frac{(2\pi n)}{N_p} \quad \text{for } n = 1, 2 \ldots\ldots (N_p-1) \tag{8.2}$$

with a prechosen v_1 based on symmetry and preferred configuration of N_p = even or odd.

In addition to the distribution of large number of N_p peakers as described above, one could also estimate a coupling parameter δ which is indicative of how well the Marx is shielded by the peakers. This factor δ is derived below and becomes more accurate as N_p increases. Consider an experiment where the Marx current $\tilde{I}_M = 0$ and we inject a total peaker current $\tilde{I}_p$ on the peakers. We then have

$$\frac{d}{dz}\ \tilde{V}_p = -\ s\mu\ f_{g_p}\ \tilde{I}_p$$

$$\frac{d}{dz}\ \tilde{V}_M = -\ s\mu\ f_{g_{PM}}\ \tilde{I}_p \tag{8.3}$$

Since the Marx has no current, the Marx voltage is nearly the same as the peaker voltage except for a small fraction, i.e.

$$\tilde{V}_M = \tilde{V}_P (1 - \delta) \tag{8.4}$$

leading to

$$\frac{d\tilde{V}_M}{dz} = (1 - \delta) \frac{d\tilde{V}_P}{dz} \tag{8.5}$$

Using the above in (8.3) gives

$$\frac{f_{g_{PM}}}{f_{g_P}} = (1 - \delta) \tag{8.6}$$

or

$$\delta = \left(1 - \frac{f_{g_{PM}}}{f_{g_P}}\right) \tag{8.7}$$

Using the results in figure 15 of [16], and assuming that the spacing between peakers is small compared to r_p so that a planar approximation is applicable, we obtain

$$\frac{\tilde{V}_M}{\tilde{V}_P} = (1 - \delta) = \frac{u_P}{u_{PO}}$$

$$\delta = \left(1 - \frac{u_P}{u_{PO}}\right) = \frac{u_{PO} - u_P}{u_{PO}} \tag{8.8}$$

$$= \frac{2\pi\Delta f_P}{u_{PO}} = \frac{\Delta f_P}{f_P}$$

δ is easily computed from the following set of equations

$$
\begin{aligned}
f_p &= (u_{PO}/2\pi) = (Z_p/Z) \\
\Delta f_p &= (u_{PO} - u_p)\ 2\pi
\end{aligned}
\tag{8.9}
$$

with

$$
\begin{aligned}
u_{PO} &= (2\pi Z_p/Z) = 2\pi\ f_p \\
u_p &= \text{arccsch}\ (r_p) \\
r_p &= \text{csch}\ (u_{PO}) \\
\Delta r &\cong \frac{r_o}{N_p}\ \ell n \left(\frac{r_o}{N_p\ r_{PA}} \right)
\end{aligned}
\tag{8.10}
$$

The geometry for the above calculations is shown in figure 8.1 and δ is shown plotted in figure 8.2 as a function of $f_p = (Z_p/Z)$ for different values of N_p. Note that Z_p is the characteristic impedance for matching between peakers and ground plane. Smaller values of δ indicate better or improved Marx shielding by peakers. The results of figure 8.2 are strictly valid for large N_p approximation (until the peaker arms approach each other to distances comparable to their individual radii), but nevertheless they should be reasonably accurate for the larger N_p chosen. Such results are useful in the process of determining an optimum number N_p, when used in configuration with wave transport calculations, across the Marx/peaker system.

Next, we may consider a case of $N_p = 8$ for example. The optimal peaker locations will be as indicated in figure 8.3. It is observed that the distribution of peakers is denser underneath the Marx and becomes sparce as one moves away from the ground plane.

In concluding this section, we observe that in the limit of large N_p approximation, the determination of optimal peaker locations simplifies and, it is possible to define and compute a coupling parameter δ which is indicative of how well the Marx column is shielded by the peakers. An illustrative example of $N_p = 8$ is also presented in this section.

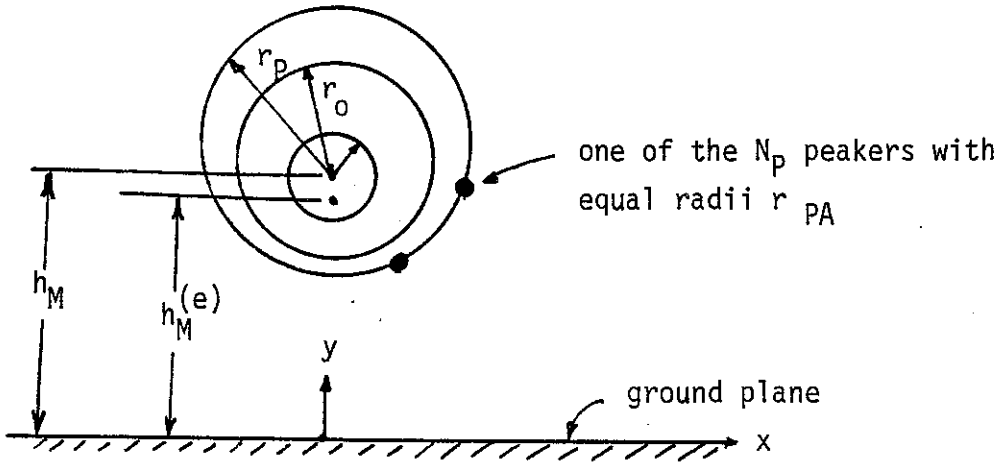

Figure 8.1 Geometry of Marx and peakers distribution.

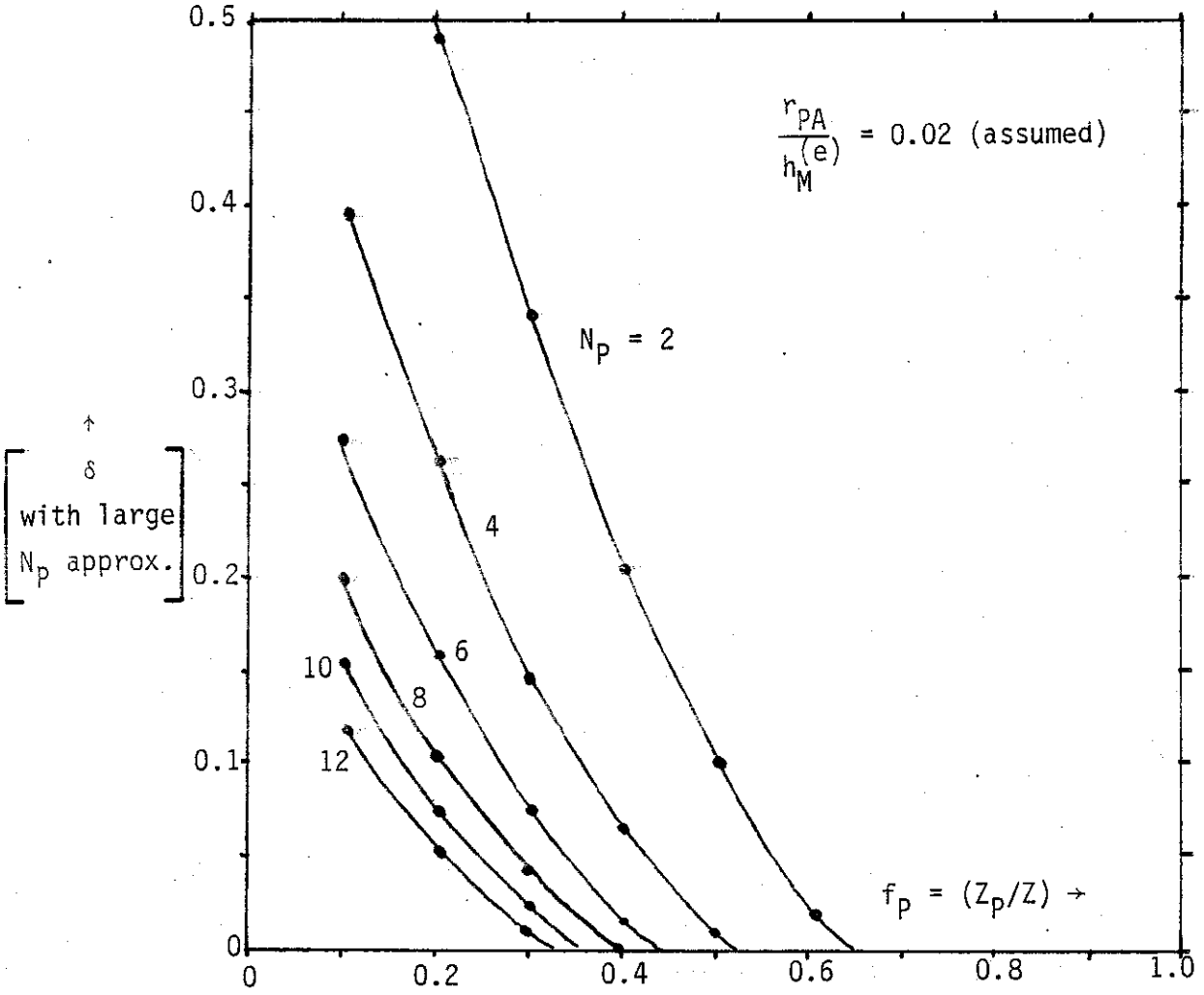

Figure 8.2 The error δ indicative of the shielding of the Marx by N_p peakers for an assumed set of normalized dimensions and a free space medium.

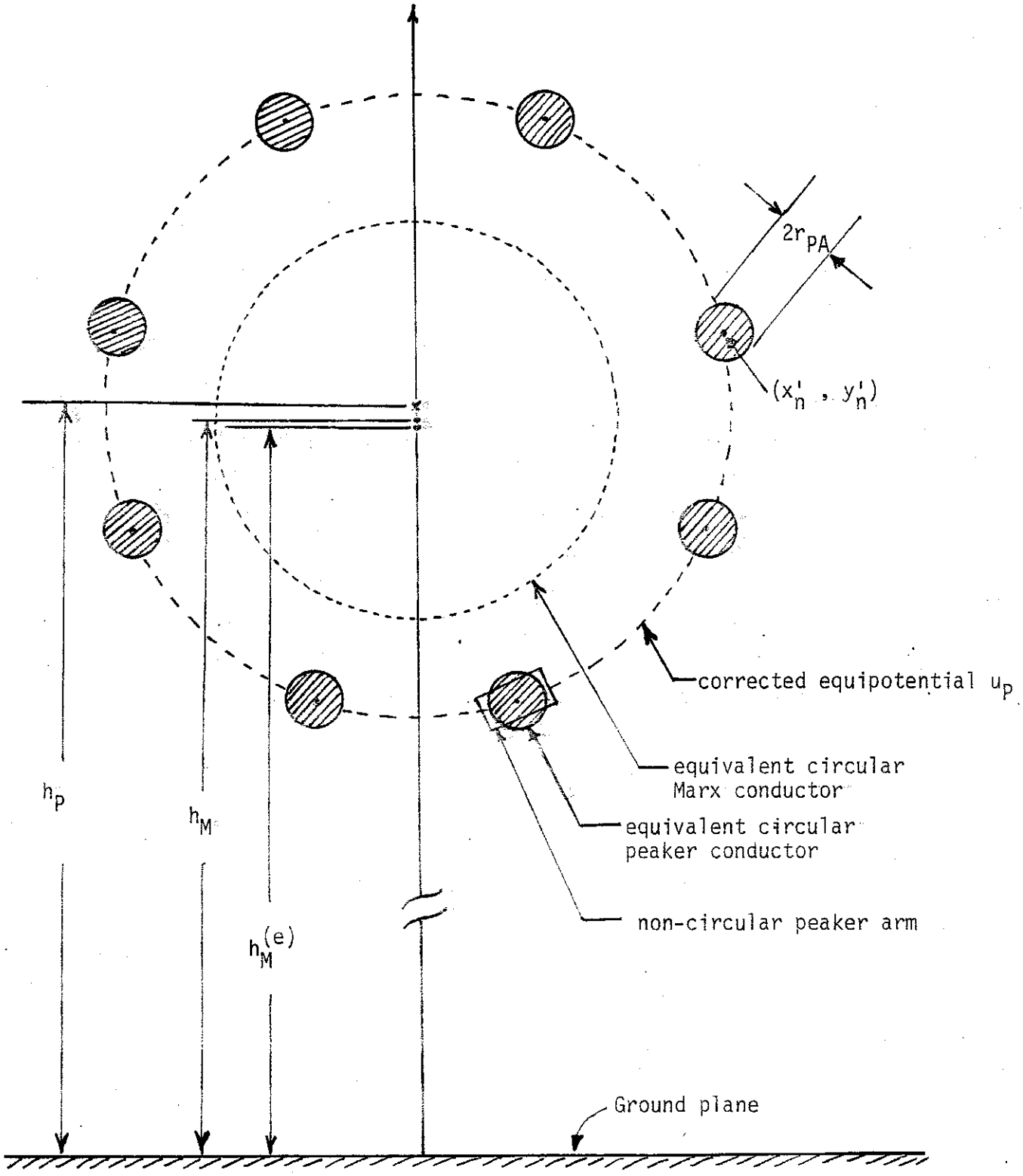

Figure 8.3 An illustration of the optimal distribution of 8 peakers around the Marx.

IX. SUMMARY

In designing pulsers for EMP simulators one is often faced with the problem of distributed peaking-capacitor design. This peaking-capacitor system not only has a circuit role in decreasing the rise time of the output pulse, but also an electromagnetic function to serve as a boundary for the fast output wave, isolating this wave from the inductive Marx generator.

To achieve optimal shielding of the Marx and reduce oscillation between the different peaker arms, constraints are imposed to assure equal voltages and currents on all peaker arms. Based on a two-dimensional model (a transmission-line approximation) optimal positions for the peaker arms meeting these constraints are derived. For the case of a large number of peaker arms this problem simplifies to the use of a conformal transformation with a correction for the peaker-arm spacing. This spacing allows some coupling between Marx and ground plane at high frequencies which can be simply approximately quantified.

REFERENCES

1. C.E. Baum, "EMP Simulators for Various Types of Nuclear EMP Environments: An Interim Categorization," Sensor and Simulation Note 240, January 1978 and Joint Special Issue on the Nuclear Electromagnetic Pulse, IEEE Trans. on Antennas and Propagation, January 1978, pp. 35 - 53, and IEEE Trans. on Electromagnetic Compatibility, February 1978, pp. 35 - 53.

2. C.E. Baum, D.V. Giri and R.D. Gonzalez, "Electromagnetic Field Distribution of the TEM Mode in a Symmetrical Two-Parallel-Plate Transmission Line," Sensor and Simulation Note 219, 1 April 1976.

3. L. Marin, "Modes on a Finite-Width, Parallel Plate Simulator, I. Narrow Plates," Sensor and Simulation Note 201, September 1974.

4. T. Itoh and R. Mittra, "Analysis of Modes in a Finite-Width Parallel Plate Waveguide," Sensor and Simulation Note 208, January 1975.

5. L. Marin, "Modes on a Finite-Width, Parallel-Plate Simulator, II. Wide Plates," Sensor and Simulation Note 223, March 1977.

6. F.C. Yang and L. Marin, "Field Distributions on a Two-Conical-Plate and a Curved Cylindrical-Plate Transmission Line," Sensor and Simulation Note 229, September 1977.

7. I.D. Smith and H. Aslin, "Pulsed Power for EMP Simulators," Joint Special Issue on the Nuclear Electromagnetic Pulse, IEEE Trans. on Antennas and Propagation, January 1978, pp. 53 - 59, and IEEE Trans. on Electromagnetic Compatibility, February 1978, pp. 53 - 59.

8. D.V. Giri, T.K. Liu, F.M. Tesche and R.W.P. King, "Parallel Plate Transmission Line Type of EMP Simulators: A Systematic Review and Recommendations," Sensor and Simulation Note 261, April 1980.

9. R.W. Latham, M.I. Sancer and A.D. Varvatsis, "Matching a Particular Pulser to a Parallel-Plate Simulator," Circuit and Electromagnetic System Design Note 18, November 1974.

10. C.E. Baum, T.K. Liu and F.M. Tesche, "On the Analysis of General Multiconductor Transmission-Line Networks," Interaction Note 350, November 1978.

11. W.R. Smythe, Static and Dynamic Electricity, McGraw Hill Book Company, Inc., New York 1950.

12. C.E. Baum, "Impedances and Field Distributions for Symmetrical Two-Wire and Four-Wire Transmission Line Simulators," Sensor and Simulation Note 27, 10 October 1966.

13. C.R. Paul and A.E. Feather, "Computation of the Transmission-Line Inductance and Capacitance Matrices from the Generalized Capacitance Matrix," IEEE Trans. on Electromagnetic Compatibility, Vol. EMC-18, No. 4, pp. 175 - 183, November 1976.

14. C.E. Baum, "Electromagnetic Topology: A Formal Approach to the Analysis and Design of Complex Electronic Systems," Interaction Note 400, Sept. 1980, and Proc. 4th Symposium on EMC, Zurich, March 1981, pp. 209-214.

15. A.K. Agrawal, H.M. Fowles and L.D. Scott, "Experimental Characterization of Multiconductor Transmission Lines in Inhomogeneous Media Using Time Domain Techniques," Interaction Note 332, February 1978.

16. C.E. Baum, "Impedances and Field Distribution for Parallel Plate Transmission-Line Simulators," Sensor and Simulation Note 21, 6 June 1966.